Scaling properties of an inviscid mean-motion fluid model

B.T. Nadiga

Earth and Environmental Sciences, MS-B296, Los Alamos National Laboratory, Los Alamos, NM 87545

An inviscid two-dimensional fluid model with nonlinear dispersion that arises simultaneously in coarse-grained descriptions of the dynamics of the Euler equation and in the description of non-Newtonian fluids of second grade is considered. The scaling of the equilibrium states of this model for conserved energy and enstrophy retains the corresponding scaling for the Euler equations on the large scales and at the same time greatly deemphasizes the importance of small scales. This is the first *clear* demonstration of the beneficial effect of nonlinear dispersion in the model, and should highlight its utility as a subgrid model in more realistic situations.

I. INTRODUCTION

In 1998, Holm et al.,[1] using the Euler-Poincaré variational formalism, proposed a model for the mean motion of ideal incompressible fluids. In this approach, the (reduced) Lagrangian, which for the incompressible case is the kinetic energy, was modified from that for the Euler equation:

$$l = \frac{1}{2} \int |\mathbf{u}|^2 \, d\mathbf{x} \; (= E) \, ,$$

to account for fluctuation energy of the velocity field in conjunction with the introduction of a fluctuation length scale α:[2]

$$l = \frac{1}{2} \int \left(|\mathbf{u}|^2 + \alpha^2 |\nabla \mathbf{u}|^2 \right) d\mathbf{x} \; (= E^\alpha) \, . \tag{1}$$

The resulting "α-model" for the Euler equations is

$$\frac{\partial \mathbf{v}}{\partial t} + \mathbf{u} \cdot \nabla \mathbf{v} - \alpha^2 \left(\nabla \mathbf{u} \right)^T \cdot \nabla^2 \mathbf{u} = -\nabla p$$

$$\nabla \cdot \mathbf{u} = 0, \quad \mathbf{v} = \left(1 - \alpha^2 \nabla^2 \right) \mathbf{u} \tag{2}$$

where, when α is set to zero, $\mathbf{v} = \mathbf{u}$, and the usual Euler equations are recovered. All other notation is standard. These equations are envisaged as modeling the flow of inviscid incompressible fluids at length scales larger than α. (For proof of existence and uniqueness of solutions of (2), see Shkoller[3] and Cioranescu & Girault[4] (viscous case).)

Rivlin and Ericksen,[5] in 1955, derived general constitutive laws of the differential type for an incompressible fluid, wherein at the first order, viscous Newtonian stress results (first grade fluids), while at the next order inviscid, non-Newtonian, stress-strain relations appear (second grade fluids). Equations (2) are identically the equations governing *inviscid* second-grade fluids, and where now α is a material property. Viscous and inviscid second grade fluid flows have since been studied from different viewpoints (e.g., see Dunn & Fosdick[6] and references therein, and Cioranescu & Girault[4]). We also note that the variational formulation of (2) was already *explicitly* noted in Cioranescu & Ouazar.[7]

The new derivation of (2) has, however, renewed interest in them and besides spurring more mathematical work has stimulated computational investigations of α-models[(e.g., 8–10)] for the reason that the advection velocity, $\mathbf{u}$, is obtained by a spatial-average of the advected field $\mathbf{v}$ (inversion of the Helmholtz operator in (2)). This results in a modification of the advective nonlinearity, the main nonlinearity of fluid dynamics, in such a way as to suppress mutual interactions between scales which are smaller than α (as can be seen, for example, in the untruncated version of (5) below when $|m|, |n| > 2\pi/\alpha$). This modification is purely inviscid, and we will refer to it simply as *nonlinear-dispersion* in what follows. However, with the exception of Nadiga & Shkoller,[10] computational studies of α-models have always used additional viscous terms: For example, Chen et al.[8] (1998) examine the applicability of a viscous α-model to model turbulent channel flow, and Chen et al.[9] (1999) explore the utility of a three-dimensional viscous α-model in providing a subgrid model for fluid turbulence. While this is clearly the appropriate direction to pursue in the context of realistic applications, we think that studying purely inviscid α-models, although idealized, is important and will complement the study of their viscous counterparts. In Nadiga and Shkoller,[10] among other things, we presented a series of two-dimensional numerical computations comparing the solutions of Euler equations, Navier-Stokes equations, and an Euler-α model, and showed that the Euler-α model was able to reproduce the typical enstrophy decay characteristics of the Navier-Stokes equations, but in a *conservative* setting. Presently, we address some statistical scaling aspects of the dynamics of such an Euler-α model to highlight its *inviscid* subgrid-scale modeling features.

To better illustrate the effects of *nonlinear-dispersion*, the salient feature of all α-models, it suffices to consider (2) in two-dimensions. In that case, it can be rewritten in the vorticity-streamfunction formulation as

$$\frac{dq}{dt} = \frac{\partial q}{\partial t} + J[\psi, q] = 0$$

$$q = \left(1 - \alpha^2 \nabla^2 \right) \omega, \quad \nabla^2 \psi = \omega, \tag{3}$$

where ψ is the streamfunction, ω is the vorticity, J is the Jacobian operator so that $J[\psi, q] = -\frac{\partial \psi}{\partial y} \frac{\partial q}{\partial x} + \frac{\partial \psi}{\partial x} \frac{\partial q}{\partial y}$, and again, when α is set to zero, $q = \omega$, and the usual Euler

equations result. Equation (3) can be also be written as

$$\frac{\partial \omega}{\partial t} + \left(1 - \alpha^2 \nabla^2\right)^{-1} J\left[\psi, \left(1 - \alpha^2 \nabla^2\right) \omega\right] = 0, \quad \nabla^2 \psi = \omega,$$

a form that highlights the modification to the $J[\psi, \omega]$ nonlinear term of the Euler equations. Parenthetically, we note that in going to two-dimensions, we lose analogs of three-dimensional processes like vorticity stretching, and therefore, fail to characterize the effect of *nonlinear-dispersion* on such processes.

The kinetic energy E^α (denoted by E when $\alpha = 0$), as defined in (1), is an obvious constant of motion in both two and three dimensions. However, in two dimensions, unlike in three, the vorticity q (ω when $\alpha = 0$) of each fluid element is an inviscid constant (see (3)), implying an infinity of conservation laws. In particular, enstrophy Z^α, defined as

$$Z^\alpha = \frac{1}{2} \int \left[\left(1 - \alpha^2 \nabla^2\right) \omega\right]^2 d\mathbf{x}, \qquad (4)$$

is a second conserved quadratic quantity. As before, when $\alpha = 0$, we represent the conserved enstrophy by Z. (The domain integral of $\mathbf{u} \cdot \boldsymbol{\omega}$ or helicity is a quadratic quantity which is conserved in three dimensions, but which is identically zero in two dimensions.)

The use of equilibrium statistical mechanical theories (for (3) with $\alpha = 0$) to better understand the inviscid dynamics of two-dimensional flows range from the two-constraint theory (see Kraichnan and Montgomery[11] and references therein) for finite truncations of the continuous system, to those based on point vortices (again see Kraichnan and Montgomery[11] and references therein) and their generalizations to continuous vorticity fields[12,13] which consider the infinity of conserved quantities. In this article, we present the two-constraint theory for (3) and verify the main results of the theory computationally. Other than mentioning that there is already some numerical evidence[10] which seems to suggest that individual solutions of the Euler-α model (3) may indeed follow predictions made for the behavior of the ensemble-averaged solutions of the Euler equations by the more complicated statistical theories we do not consider such theories any more in this short note. Also, since one may be tempted to point to the shortcomings of the two-constraint theory for the Euler equations before considering the utility of such a theory for the Euler-α model, we wish to point out that the importance of this work lies primarily in the comparison of the results for the Euler-α model to the classical results for the Euler equations. In so doing, the effects of *nonlinear-dispersion*, and its beneficial numerical ramifications, are clearly highlighted. At the risk of belaboring the point further, we reemphasize that in considering the simple two constraint theory, we are in no way suggesting that the behavior of the ensemble averaged solution of the α-model (3) (or their slightly viscous counterparts) will follow this theory in more realistic situations; the limitation of this theory in predicting

large-scale coherent structures in the $\alpha = 0$ case is well known,[11] and carry over to the nonzero α case.

Furthermore, from a numerical point of view, inviscid computations of (3) which conserve two quadratic invariants are fairly easily realizable and more common-place than the more involved multisimplectic schemes which are required for conserving a larger number of constraints. Also, while state of the art schemes of the latter kind can handle only tens of modes (because of an $N^3 \log N$ scaling of computational work, where, N is the number of modes[14]), there is no such restriction on schemes of the former kind. Examples of schemes which conserve just the energy and enstrophy invariants are Fourier-Galerkin truncations implemented as a fully dealiased pseudospectral spatial discreteization and the second-order finite difference spatial discreteization using the Arakawa Jacobian. While we have done computations with both these schemes and see no discrepancy between the results, we consider only the spectral discretization in this article since the theory presents itself most naturally in this setting.

II. TWO-CONSTRAINT STATISTICAL THEORY FOR (3)

Let $q_{\mathbf{x}}$ represent a discretization of q on a two-dimensional spatial grid, $\mathbf{x}$, with $2N+1$ equispaced points on each side. Let $\widehat{q}_{\mathbf{k}}$, where $\mathbf{k}$ is the set of all wave-vectors $k = (k_x, k_y)$ denote the Fourier transform of $q_{\mathbf{x}}$. Although there are $(2N + 1)^2$ k-space grid points, since $q_{\mathbf{x}}$ is real, not all of them are independent and $\widehat{q}_k = \widehat{q}_{-k}^*$. Therefore, there are only half as many k-space grid points, and, $\mathbf{k}$ the set of all k is such that

$$\mathbf{k} \equiv \left\{k = (k_x, k_y), \quad k_{min} \leq k_x, k_y \leq k_{max}\right\}.$$

However, since each $\widehat{q}_k$ is a complex number, there are overall $(2N + 1)^2$ degrees of freedom in $\widehat{q}_{\mathbf{k}}$. Consider the truncation of (3) that is closed in $\widehat{q}_{\mathbf{k}}$:

$$\frac{d}{dt}\widehat{q}_k + \sum_{\substack{m+n=k \\ k,m,n \in \mathbf{k}}} \widehat{q}_m \widehat{q}_n \frac{m \times n}{|m|^2 \left(1 + \alpha^2 |m|^2\right)} = 0. \qquad (5)$$

Among the infinity of conservations for the continuous system (3) previously discussed, conservations (1) and (4) are the only ones which survive for the truncated system (5), and may be expressed in terms of $\widehat{q}_k$ as

$$E^\alpha = \frac{1}{2} \sum_{k \in \mathbf{k}} \frac{|\widehat{q}_k|^2}{|k|^2(1 + \alpha^2 |k|^2)}, \quad Z^\alpha = \frac{1}{2} \sum_{k \in \mathbf{k}} |\widehat{q}_k|^2. \quad (6)$$

This follows from the *detailed* conservation property of energy and enstrophy wherein each of these quantities is conserved in every triad interaction.

Considering the dynamics of $\widehat{q}_{\mathbf{k}}$ under (5), we work in the $(2N + 1)^2$ dimensional phase space. As a consequence of (3) satisfying a *detailed* Liouville theorem (see

Kraichnan and Montgomery[11] and references therein), (5) also satisfies a Liouville theorem and the motion of $\widehat{q}_\mathbf{k}$ in the truncated phase space is divergence free.[11] We can, therefore, define a stationary probability density, P, such that $P \prod_{k \in \mathbf{k}} d\widehat{q}_k$ is the probability of finding the system within the $((2N+1)^2$ dimensional) phase space volume $\prod_{k \in \mathbf{k}} d\widehat{q}_k$ centered around $\widehat{q}_\mathbf{k}$, and the ensemble average of any quantity O, a function of $\widehat{q}_\mathbf{k}$, as

$$\langle O \rangle = \int OP \prod_{k \in \mathbf{k}} d\widehat{q}_k. \tag{7}$$

Next, a maximization of the information theoretic entropy s, defined in the usual fashion as

$$s = -\langle \ln P - 1 \rangle = -\int (P \ln P - P) \prod_{k \in \mathbf{k}} d\widehat{q}_k,$$

subject to constant ensemble-averaged energy and enstrophy, $\langle E^\alpha \rangle$ and $\langle Z^\alpha \rangle$ respectively, leads to

$$P = a \exp(-\beta E^\alpha - \gamma Z^\alpha). \tag{8}$$

Here, β (an inverse temperature associated with energy) and γ (an inverse temperature associated with enstrophy) are the Lagrange multipliers associated with the two constraints, and a is determined from

$$\int P \prod_{k \in \mathbf{k}} d\widehat{q}_k = 1.$$

Making use of (6) in (8) then leads to a factorization of the probability density:

$$P = a \prod_{k \in \mathbf{k}} \exp\left(-|\widehat{q}_k|^2 \left(\frac{\beta}{|k|^2 (1 + \alpha^2 |k|^2)} + \gamma\right)\right). \tag{9}$$

The ensemble averaged two-dimensional spectral density is then computed using (7) and (9) (after noting the expressions for the moments of a Gaussian) as

$$\langle U^\alpha(k) \rangle \equiv \frac{1}{2} \langle \frac{|\widehat{q}_k|^2}{|k|^2 (1 + \alpha^2 |k|^2)} \rangle = \frac{1}{4} \frac{1}{\beta + \gamma |k|^2 (1 + \alpha^2 |k|^2)}.$$

Since (the isotropic) one-dimensional spectra are more convenient for plotting, we define

$$E^\alpha(|k|) = \sum_{|k| \le |j| < |k|+1} \langle U^\alpha(j) \rangle, \quad \text{so that} \quad E^\alpha = \sum_{|k|} E^\alpha(|k|).$$

In what follows, we drop the $|\cdot|$ sign on k and to avoid confusion, note that while E^α represents the total conserved energy, $E^\alpha(k)$, with a dependence on k, represents the corresponding one-dimensional spectrum. The one-dimensional spectrum $E^\alpha(k)$ is then seen to scale with k as

$$E^\alpha(k) \sim \frac{k}{\beta + \gamma k^2 (1 + \alpha^2 k^2)}, \tag{10}$$

with the above scaling being only approximate when the mode spacing is not small compared to k (as at small k).

In (10), since α is a given length scale, once the discretization is fixed, expressions for the total energy and enstrophy of the given initial conditions provide two equations to solve for β and γ. The equilibrium spectral scaling (10) is then seen to exhibit three regimes depending on the values of the conserved energy and enstrophy as follows. If the minimum and maximum wavenumbers of the truncation are k_{min} and k_{max} respectively, and if we define a mean wavenumber[15] of the initial conditions as,

$$k_1 = \sqrt{\frac{Z^\alpha}{E^\alpha}},$$

then, we can identify three regimes depending on the signs of β and γ:

- If the initial conditions are such that the mean wavenumber k_1 is small: $k_{min} \le k_1 < k_a$, then the temperature corresponding to energy is negative, while that corresponding to enstrophy is positive: $-\gamma k_{min}^2 (1 + \alpha^2 k_{min}^2) < \beta < 0, \gamma > 0$;

- If the mean wavenumber k_1 is medium: $k_a < k_1 < k_b$, then both temperatures are positive: $\beta > 0$, $\gamma > 0$;

- If the mean wavenumber k_1 is large: $k_b < k_1 \le k_{max}$, then the temperature corresponding to energy is positive while the temperature corresponding to enstrophy is negative: $\beta > 0$, $-\beta < \gamma k_{max}^2 (1 + \alpha^2 k_{max}^2) < 0$.

Here, k_a, and k_b are constants depending on the filter length α and the discretization:

$$k_a^2 = \frac{k_{max}^2 - k_{min}^2}{2} \left[\log\left(\frac{k_{max}(1 + \alpha^2 k_{min}^2)}{k_{min}(1 + \alpha^2 k_{max}^2)}\right)\right]^{-1},$$

$$k_b^2 = \frac{k_{max}^2 + k_{min}^2}{2} + \alpha^2 \frac{k_{max}^4 + k_{max}^2 k_{min}^2 + k_{min}^4}{3}.$$

(In the case of an infinite domain, the first of the above cases, $\beta < 0$, cannot occur since $k_a = 0$.)

Further, we can also compute the spectrum of the energy conserved by the Euler equation (E) under the dynamics of the Euler-α model. Noting that

$$E = \frac{1}{2} \sum_{k \in \mathbf{k}} \frac{|\widehat{q}_k|^2}{|k|^2 (1 + \alpha^2 |k|^2)^2},$$

(an extra factor $(1 + \alpha^2 |k|^2)$ in the denominator compared to the expression for E^α) and that E is not conserved for $\alpha \ne 0$, the scaling of its one-dimensional spectrum, denoted simply by $E(k)$, may be written as[16]

$$E(k) \sim \frac{k}{(1 + \alpha^2 k^2)(\beta + \gamma k^2 (1 + \alpha^2 k^2))}. \tag{11}$$

3

III. DISCUSSION AND COMPUTATIONAL VERIFICATION OF RESULTS

We devote the remainder of the article to a discussion of the scalings (10) and (11) and their computational verification. First, when α is set to zero in either (10) or (11), the classic result of Kraichnan[11] for the Euler equation:

$$E(k) \sim \frac{k}{\beta + \gamma k^2} \qquad (12)$$

is recovered, with the three regions corresponding to the different combination of signs for β and γ now separated by values of the mean wavenumber k_1 corresponding to k_a and k_b, where k_a and k_b are given by

$$k_a^2 = \frac{k_{max}^2 - k_{min}^2}{2} \left[\log \left(\frac{k_{max}}{k_{min}} \right) \right]^{-1}, \quad k_b^2 = \frac{k_{max}^2 + k_{min}^2}{2}.$$

As has been noted many times now[11] for $\alpha = 0$, there is no discontinuity of any sort in going from one region to the other among the three regions corresponding to different combinations of signs of β and γ. Therefore, for convenience, we first consider, in detail, the case $\beta > 0$ and $\gamma > 0$, and define

$$k_*^\alpha = \frac{1}{\alpha \sqrt{2}} \left(-1 + \sqrt{\frac{4\alpha^2 \beta}{\gamma} + 1} \right)^{\frac{1}{2}},$$

$$k_* = \lim_{\alpha \to 0} k_*^\alpha = \sqrt{\frac{\beta}{\gamma}},$$

and note that

$$k_*^\alpha = k_* \left(1 + O(\alpha^2 k_*^2) \right).$$

Furthermore, k_* can be shown[17] to be of the order of k_1. (Thus, for simplicity in what follows, one may use k_1, k_1^α, k_*, and k_*^α interchangably, or represent all of them by k_1.) For the Euler solutions, we have from (10) with $\alpha = 0$, the large scales and small scales (with respect to k_*) behaving asymptotically as

$$E(k) \sim k, \qquad k_{min} \leq k \ll k_*;$$
$$E(k) \sim k^{-1}, \quad k_* \ll k \leq k_{max}, \qquad (13)$$

implying equipartition of E at large scales and equipartition of Z at small scales. (When $k \ll k_*$, $\gamma k^2 \ll \beta$ in (12) and when $k \gg k_*$, $\gamma k^2 \gg \beta$ in (12).) When α is not zero, however, from (10), one easily sees the analogous E^α- and Z^α-equipartition results to be respectively

$$E^\alpha(k) \sim k, \qquad k_{min} \leq k \ll k_*^\alpha;$$
$$E^\alpha(k) \sim k^{-3}, \quad k_*^\alpha \ll k \leq k_{max}. \qquad (14)$$

This implies that *nonlinear-dispersion* in (3) acts in such a way as to **preserve the Euler scaling of dynamics at the large scales while at the same time greatly deemphasizing the importance of small scales**.

Asymptotic scalings arising from (11), for the nonconserved energy for $\alpha \neq 0$:

$$E(k) \sim k, \qquad k_{min} \leq k \ll k_*^\alpha;$$
$$E(k) \sim k^{-5}, \quad k_*^\alpha \ll k \leq k_{max}. \qquad (15)$$

further reinforce this result. Finally, we note that for $\alpha = 0$, it is well known[11] (and easy to see from (10)) that when $k_{max} \to \infty$, energy diverges logarithmically and enstrophy diverges quadratically. However, when $\alpha \neq 0$, one can see from (10) that when $k_{max} \to \infty$, energy is not divergent and that the enstrophy Z^α is quadratically divergent. Nevertheless, in Nadiga and Shkoller,[10] we show that it is the dynamics of the non-conserved enstrophies $\frac{1}{2} \int \omega^2 d\mathbf{x}$ and $\frac{1}{2} \int \left[(1 - \alpha^2 \nabla^2)^{\frac{1}{2}} \omega \right]^2 d\mathbf{x}$ which are actually interesting. While the former does not diverge, the latter diverges only weakly (logarithmically).

We have carried out a series of computational experiments on a doubly periodic two-dimensional domain, wherein an ensemble of initial conditions were evolved under (5) for different values of α until statistical equilibration was achieved. Initial conditions, similar to those in Fox and Orsag,[18] were obtained by choosing amplitudes for wavenumbers in the band $50 \leq |k| \leq 51$ (zero elsewhere) from a zero-mean normal distribution of random numbers. The variance was scaled in such a way that for the different values of α, the conserved energy[19] had the same value: $E^\alpha = E$. The mean wavenumber k_1 for this set of initial conditions corresponds to about 50.5, and for the resolution chosen below, $28.5 \leq k_a \leq 43.5$, and $k_b \geq 60.1$. With this setup, besides letting both β and γ be positive, we can realize both the energy and enstrophy equipartition regimes in the same experiment.

A fully dealiased pseudospectral spatial discretization was used with $k_{min} = 1$, and $k_{max} = N = 85$, and the nonlinear terms were computed in physical space using 256 grid points in each direction. A nominally fifth-order, adaptive time stepping, Runge-Kutta Cash-Karp algorithm[20] was used for time integration. Energy was conserved to better than 1 in 10^5 and enstrophy to better than 1 in 10^4 over the entire duration of the runs.

In Fig. 1, we plot the (instantaneous) spectrum $E^\alpha(k)$ against k, on a log-log scale for four different values of α: 0, 0.05, 0.10, and 0.15, corresponding to between 0 to 2.4 percent of the domain size. The spectrum for the Euler case ($\alpha = 0$) is offset by a decade so as to not clutter the figure, and slopes of 1, -1, and -3 are drawn for reference. The scalings, (13) for $\alpha = 0$, and (14) for nonzero α, are clearly verified at both large and small scales, in Fig. 1, with in fact a cleaner (but identical) scaling of the large scales for nonzero α. Furthermore, the three spectra corresponding to the nonzero-α cases seem to collapse onto a single curve in Fig. 1. This collapse may be explained by noting that almost all the energy is contained in the low-k modes (denoted below

by the set of wavenumbers $\mathbf{k}_E$) and almost all enstrophy is contained in the high-k modes (denoted below by the set of wavenumbers $\mathbf{k}_Z$). This leads to a leading order expression for β which is independent of α:

$$\beta(\alpha) \sim \sum_{\mathbf{k}_E} k/E,$$

and one for γ which is inversely proportional to α^2:

$$\gamma(\alpha) \sim \sum_{\mathbf{k}_Z} k/(\alpha^2 k_1^2 Z).$$

This in turn implies that the spectra (10) should be almost independent of α, except for a small intermediate range of k.
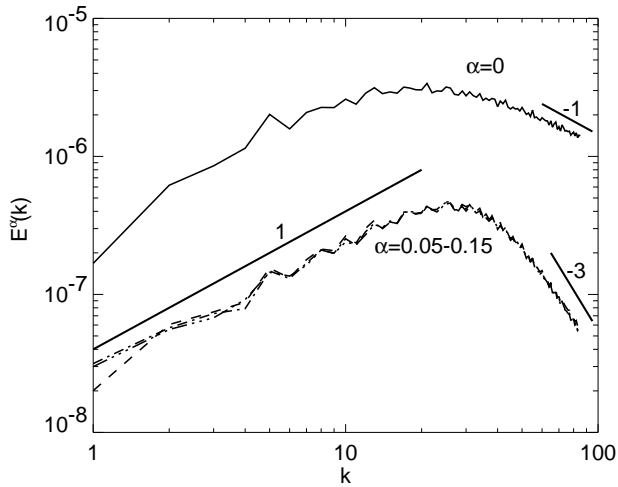

FIG. 1. Plot of $E^\alpha(k)$ vs. k for $\alpha=0$ (offset by a decade), and $\alpha = 0.05$, 0.10, & 0.15. Low-k scaling is identical for zero or nonzero α, but high-k scaling is much steeper for $\alpha \neq 0$. The theoretical asymptotic slopes are drawn for reference.

The above collapse of the nonzero-α spectra onto a single curve seems to suggest that the actual value of α is not very important as long as its value is in a certain range. This, however, is not true as can be seen from the structure of the $E(k)$ spectrum plotted in Fig. 2 for the same four cases. The theoretical scaling for this spectrum is given in (11) and the asymptotic scalings are given in (15). Although the small scale behavior is as expected, it is clear that with increasing α, the structure of the large scales is being substantially modified. (Scaling (15) at large scales, can obviously be realized by increasing the number of modes, but that is not our intent here; we are examining the effect of α at fixed resolution.) Therefore, a small value of α is indicated. In such a case, the *nonlinear-dispersion* of the α-model is highly beneficial at small-scales while the large-scale distortion is minimal. Considering that the minimally resolved length scale in these computations corresponds to about 0.074, one may conclude that α should be of

that order. That is to say, besides their use in describing second-grade fluids, α-models in general and (3) in particular should be useful as a subgrid model in under-resolved computations.
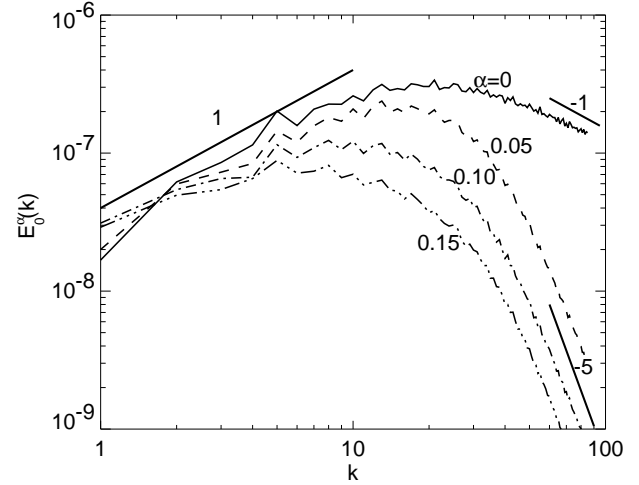

FIG. 2. Plot of $E(k)$ vs. k for $\alpha = 0$, 0.05, 0.10, & 0.15. Spectrum falls off much faster (k^{-5}) for $\alpha \neq 0$ compared to k^{-1} for $\alpha = 0$, but the large-scales are also increasingly changed with increasing α.

These conclusions are also borne out in numerical experiments corresponding to the fluid-dynamically more interesting case wherein the temperature associated with energy is negative ($\beta < 0$). As mentioned earlier, such a case is obtained when the initial conditions are chosen with energy and enstrophy such that $k_1 < k_a$. (As before, $28.5 \leq k_a \leq 43.5$ for the different values of α for the discretization chosen.) In such a case, there is a condensation of energy on to the low modes of the system[11] resulting in large scale structures (necessarily coherent). However, the enstrophy equipartition scaling of the spectra discussed previously are unchanged. This gives us an opportunity to better test the extent of distortion of the low wavenumber (coherent) modes due to increasing α. While various aspects of the negative temperature case for nonzero α are considered in Nadiga and Shkoller,[10] in the spirit of this article, we presently consider only the spectral distortion to the structure of the low wavenumber (coherent) modes. In Fig. 3, where we plot the spectrum $E(k)$ versus k again for $\alpha = 0$, 0.05, 0.10, & 0.15, and now where $k_1 \approx 2$. For this case, only one realization (for each value of α) is considered and the spectrum corresponds to a long time average, for good measure, taken after the system has reached statistical equilibrium. For this suite of runs, energy was conserved to machine precision while enstrophy was conserved to about 0.3% for the entire duration of the runs considered. The steep slope of -5, for the small scales, for nonzero α (compared to a slope of -1 for $\alpha = 0$) is again verified and more importantly, for the case of $\alpha = 0.05$, the low-mode structure (up to $k = 10$) is almost identical to the case of $\alpha = 0$.

This is clearly not the case for the two other values of the filter length, α, which are greater than the smallest resolved scale of the computation.
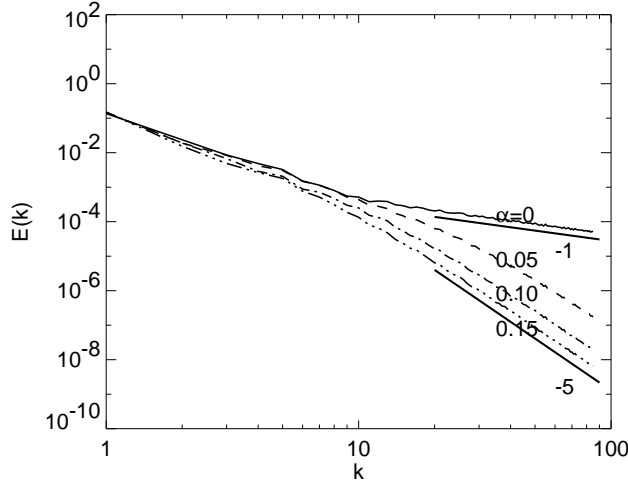

FIG. 3. Negative temperature case. Plot of $E(k)$ vs. k for $\alpha = 0$, 0.05, 0.10, & 0.15. Small-scale spectrum falls off much faster (k^{-5}) for $\alpha \neq 0$ compared to k^{-1} for $\alpha = 0$. While the large scale distortion is minimal for α=0.05, it is appreciable for the other two cases with larger α.

[1] D.D. Holm, J.E. Marsden, and T.S. Ratiu, *Euler-Poincaré models of ideal fluids with nonlinear dispersion*, Phys. Rev. Lett. **80**, 4273–4277 (1998).

[2] The integrand in (1) is slightly modified for domains with boundaries.

[3] S. Shkoller, *Geometry and curvature of diffeomorphism groups with H^1 metric and mean hydrodynamics*, J. Func. Anal. **160**, 337–365 (1998).

[4] D. Cioranescu and V. Girault, *Solutions variationnelles et classiques d'une famille de fluides de grade deux*, Comptes Rendues de l'Acad. Sci. de Paris Serie 1 **322**, 1163–1168 (1996).

[5] R.S. Rivlin and J.L. Ericksen, *Stress-deformation relations for isotropic materials*, J. Rat. Mech. Anal. **4**, 323–425 (1955).

[6] J.E. Dunn and R.L. Fosdick, *Thermodynamics, stability and boundedness of fluids of complexity 2 and fluids of second grade*, Arch. Rat. Mech. Anal. **56**, 191–252 (1974).

[7] D. Cioranescu and E.H. Ouazar, *Existence et unicit'e pour les fluides de second grade*, Comptes Rendues de l'Acad. Sci. de Paris Serie 1 **298**, 285–287 (1984).

[8] S. Chen, C. Foias, D.D. Holm, E. Olson, E. S. Titi,
and S. Wynne, *The Camassa-Holm equations as a closure model for turbulent channel flow*, Phys. Rev. Lett. **81**, 5338–5341 (1998).

[9] S. Chen, D.D. Holm, L. Margolin, and R. Zhang, *Direct numerical simulations of the Navier-Stokes alpha model*, preprint (1999).

[10] B.T. Nadiga and S. Shkoller, *Mean motion, second-grade fluids, and the vortex-blob method*, preprint (1999).

[11] R.H. Kraichnan and D. Montgomery, *Two-dimensional turbulence*, Rep. Prog. Phys. **43**, 547–619 (1980).

[12] R. Robert and J. Sommeria, *Statistical equilibrium states for two-dimensional flows*, J. Fluid Mech. **229**, 291–310 (1991).

[13] J. Miller, P.B. Weichman, and M.C. Cross, *Statistical-mechanics, Euler equation, and Jupiter red spot*, Phys. Rev. A **45**, 2328–2359 (1992).

[14] S. Shkoller, personal communication.

[15] We can define $k_1^\alpha = \sqrt{\frac{Z^\alpha}{E^\alpha}}$, and $k_1 = \sqrt{\frac{Z}{E}}$. Then $k_1^\alpha = k_1 \left(1 + O(\alpha^2 k_1^2)\right)$. Since the exact value of k_1 is not crucial, to keep things simple, we use k_1 for k_1^α also.

[16] Similarly also, the one-dimensional spectrum of $\frac{1}{2}\sum_{k \in \mathbf{k}} \frac{|\widehat{q_k}|^2}{|k|^2}$ (again not conserved for $\alpha \neq 0$) scales as $\frac{k\left(1+\alpha^2 k^2\right)}{\beta + \gamma k^2\left(1+\alpha^2 k^2\right)}$.

[17] C. Basdevant and R. Sadourny, *Ergodic properties of inviscid truncated models of two-dimensional incompressible flows*, J. Fluid Mech. **69**, 673–688 (1975).

[18] D.G. Fox and S.A. Orszag, *Inviscid dynamics of two-dimensional turbulence*, Phys. Fluids **16**, 169–171 (1973).

[19] This results in the scaling of the conserved enstrophy Z^α with α as $Z^\alpha \approx Z(1 + \alpha^2 k_1^2)$.

[20] W.H. Press, B.P. Flannery, S.A.Teukolsky, and W.T. Vetterling, *Chapter 16*, Numerical Recipes in Fortran 77, Cambridge University Press, 708–716 (1992).